Influence of carrier density on the friction properties of silicon *pn* junctions

Jeong Young Park,[1,*,†] Yabing Qi,[1] D. F. Ogletree,[1] P. A. Thiel,[2] and M. Salmeron[1,*,‡]
[1]*Materials Sciences Division, Lawrence Berkeley National Laboratory, University of California, Berkeley, California 94720, USA*
[2]*Ames Laboratory and Departments of Chemistry and of Materials Science and Engineering, Iowa State University, Ames, Iowa 50011, USA*

(Received 11 May 2007; revised manuscript received 22 June 2007; published 13 August 2007)

We present experimental results showing a significant dependence of the friction force on charge carrier concentration in a Si semiconductor sample containing *p*- and *n*-type regions. The carrier concentration was controlled through application of forward or reverse bias voltages in the *p* and *n* regions that caused surface band bending in opposite directions. Excess friction is observed only in the highly doped *p* regions when in strong accumulation. The excess friction increases with tip-sample voltage, contact strain, and velocity. The sample is an oxide-passivated Si (100) wafer patterned with arrays of 2-μm-wide highly doped *p*-type strips with a period of 30 μm in a nearly intrinsic *n*-type substrate. The countersurface is the tip of an atomic force microscope coated with conductive titanium nitride. The excess friction is not associated with wear or damage of the surface. The results demonstrate the possibility of electronically controlling friction in semiconductor devices, with potential applications in nanoscale machines containing moving parts.

DOI: 10.1103/PhysRevB.76.064108 PACS number(s): 46.55.+d, 68.37.Ps, 73.40.Qv, 81.40.Pq

I. INTRODUCTION

The nature of the fundamental processes that give rise to friction between sliding bodies in close proximity is a long-standing question in tribology, both theoretically and experimentally.[1–3] Energy is dissipated by conversion of kinetic energy of the moving bodies into lattice vibrations or phonons (heat). Even before contact is established, fluctuating electric fields emanating from charges in the two bodies exert forces on each other that produce work (dissipation-fluctuation theorem). During contact, more direct interactions can take place, which can be described as follows. First, the atoms on each side of the interface rearrange elastically to positions that minimize their interaction energy with the surrounding atoms. As the surfaces are translated, interface atoms are displaced away from these minima. Unless the potential is very weak, the atomic displacement consists of irreversible jumps over the potential barriers that leave atoms vibrating at their natural frequencies. This is the essence of the Tomlinson model of friction.[4] In atomic force microscopy (AFM), the atomic jumps produce stick-slip events with lattice periodicity when one of the surfaces is crystalline.[5] The vibrations of the surface atoms are damped by energy transfer to the bulk material through propagating phonon modes and in metals also by electronic excitations. Although direct creation of electron-hole pairs has been invoked as a mechanism of frictional energy dissipation,[1,6–15] the importance of this dissipation channel has not been determined experimentally. Besides the weaker effect of fluctuating fields, phonon creation is the predominant damping mechanism in insulators, while in metals excitation mechanisms involving conduction electrons can also contribute.

Semiconductors offer the interesting possibility to test the effect of free charge carriers on the energy dissipation because it is possible to reversibly change the charge density near the surface over many orders of magnitude. We tested this idea by performing experiments on a substrate, where the density of free charge carriers can be changed in a spatially controlled manner.[15] In this experiment, we used an AFM tip coated with conductive TiN sliding on a silicon sample patterned with *p* and *n* regions of different doping levels.[15] Friction was monitored as a function of carrier accumulation or depletion, which was controlled by application of a bias voltage to the tip. While the *p* and *n* regions of the sample have different electronic properties, their chemical nature and structure are the same, due to a thin oxide layer covering both regions. This layer also prevents Fermi level pinning, which could obscure dopant-dependent contrast in the conductance.[16,17] In this paper, we present more detailed experimental results and discuss possible mechanisms responsible for this finding. Specifically, we present results on the dependence of the "excess" friction in the highly doped regions on bias voltage, scanning velocity, and on the presence of additional passivating layers on the AFM probe.

II. EXPERIMENT

An array of *p*-type stripes located at 30 μm intervals was fabricated by boron implantation at 190 keV into an *n*-type Si (100) substrate with a low dopant (phosphor) concentration of 1.6×10^{14} cm^{-3}. The nominal depth of the implanted stripes was 0.7 μm with a boron concentration of 5×10^{18} cm^{-3}. The surface was prepared by wet chemical oxidation using the Shiraki procedure.[16,18] The oxide layer is thought to be between 0.3 and 1 nm thick, as shown in a previous scanning tunneling microscopy (STM) study.[16] The lateral distribution of carrier density and potential across the *pn* junction has been studied with STM and conductance mapping.[19,20] Figure 1(a) shows a 45×45 μm^2 topographic image of *pn* junction stripes acquired with AFM in tapping mode. Small protrusions and depressions ($\sim$0.7 nm deep) mark the boundary between *n* and *p* stripes. They are the result of the etching procedures used in fabricating the ion implantation mask. Figure 1(b) shows a 2.0×2.0 μm^2 topographic image of the *pn* junction. As can be seen, there is no difference in the morphology between the *p* and *n* regions,

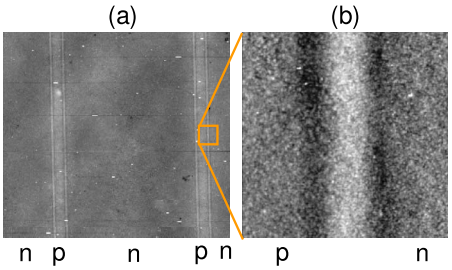

FIG. 1. (Color online) (a) 45×45 μm^2 topographic image showing *pn* junction stripes patterned on a Si (100) sample. The images were acquired with AFM in tapping mode. (b) 2.0×2.0 μm^2 expanded showing the smooth oxide morphology on both *p* and *n* regions.

indicating that the oxide formed on both regions is uniform.

The friction experiments were performed with an STM/AFM system[21] in a chamber with a base pressure in the 10^{-10} torr range.[22,23] We used cantilevers with nominal spring constants of 2.5 N/m coated with approximately 50 nm of TiN, which is hard and conducting.[24] The normal force was kept constant during imaging, while current and friction force were simultaneously recorded. The sample was mounted with a common electrical contact to both *p* and *n* regions. The loads used in this study were sufficiently small that neither the tip nor the surface was damaged. No wear traces were observed in repeated high-resolution images, and the friction and adhesion measurements were reproducible

To determine forces, the cantilever spring constant was calibrated using the method of Sader *et al.*,[25] while the lateral force was calibrated with the method of Ogletree *et al.*[26] The radii of the metal-coated tips were 30–50 nm before contact, as measured by scanning electron microscopy. When measured after a contact experiment, however, the radii were found to be 80–120 nm. Since the measured friction force did not change at a constant load and did not show a time-dependent behavior in the elastic regime, we assume that the changes in the tip radius took place soon after the first contact, with minimum changes during subsequent contact measurements.

III. RESULTS

Figures 2(a) and 2(b) show 4.0×5.0 μm^2 topographic and friction images of the *pn* junction acquired at an applied load of 35 nN and sample bias of 0 V. Topographic and friction force profiles across the junction are shown in Fig. 2(c). As can be seen, there is no difference in friction between the *p* and *n* regions within the noise level of the measurement. The friction force is shown as a function of load in Fig. 2(d), along with a fit to the Derjaguin-Müller-Toporov (DMT) and Johnson-Kendall-Roberts (JKR) contact models for a tip radius of 100 nm.[27] The fit assumes the friction to be proportional to the contact area. The agreement with the DMT model is excellent, consistent with the high stiffness of TiN and silicon.[28,29]

When a voltage is applied between the sample and tip, band bending takes place, which changes the electrical character of the *p* and *n* regions in opposite directions. When a positive voltage is applied to a *p*-type semiconductor, the top of the valence band shifts downward and may cross the Fermi level near the surface.[20,30] Since the carrier density depends exponentially on the energy difference between the Fermi level and valence band edge, this band bending causes accumulation of majority carriers (holes) near the semiconducting surface. When a negative voltage is applied, the bands shift upward and carriers are depleted near the surface.

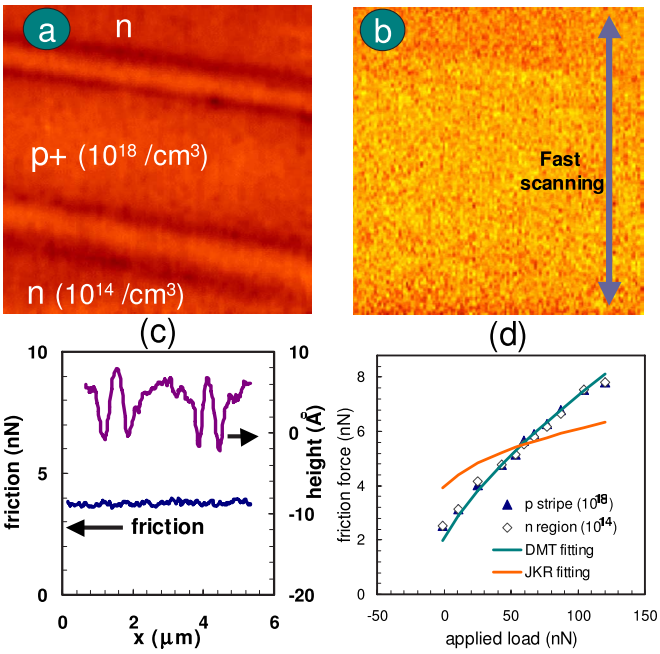

FIG. 2. (Color online) (a) 4.0×5.0 μm AFM topographic and (b) friction images across the *p* and *n* regions of the sample. Tip-sample bias was 0 V and the applied load was 35 nN. (c) Topography and friction profiles across the *pn* junction. The friction profile shows no difference between the *p* and *n* regions. (d) Plot of measured friction in *p* and *n* regions versus applied load at 0 V bias and scanning speed of 5 $\mu m/s$. The solid curve is a fit to the DMT contact model. The predictions of the Johnson-Kendall-Roberts (JKR) model are also shown for comparison.

Figure 3 shows (a) topographic, (b) current, and (c) friction images at a sample bias of +4 V. Figure 3(d) is the line profile of Figs. 3(b) and 3(c) across the *pn* junction. The highly doped *p* region is forward biased and in strong accumulation, leading to a high carrier concentration near the surface.[20,30] The *n* region is reverse biased, causing depletion or weak inversion. As a result, the current was high in the *p* region (~50 μA) and low in the *n* region (~5 μA), as shown in Fig. 3(d). Remarkably, friction was significantly higher in the *p* region than in the *n* region, as shown in Figs. 3(c) and 3(d).

Figure 4 also shows images of the (a) topography, (b) current, and (c) friction at the opposite sample bias of −4 V. Figure 4(d) is the line profile of Figs. 4(b) and 4(c) across the *pn* junction. In this case, the *n* region is forward biased, while the *p* region is in inversion. The current in the *n* region was higher (~10 μA) than in the *p* region (~6 μA), as shown in the line profile in Fig. 4(d). The depletion layer between the *p* and *n* regions is also visible and shows an

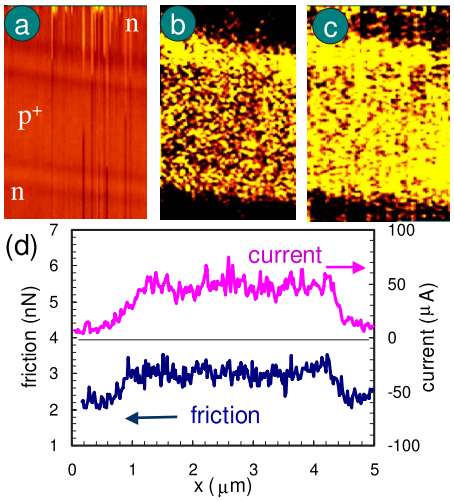

FIG. 3. (Color online) (a) 3.5×5.0 μm topography, (b) current, and (c) friction images of a region containing a stripe of p-type Si at +4 V bias. Bright corresponds to high values, and dark to low values. The p region is forward biased (strong accumulation), and the n region reverse biased. The applied load was 8 nN and the scanning speed was 5 μm/s. (d) Line profiles of current and friction across the pn junction. [Reprinted with permission from Science (http://www.aaas.org), Ref. 15. Copyright 2006 AAAS.]

even lower current (<0.2 μA). Interestingly, no significant variation of friction force was observed between the n and p regions at negative bias.

Figures 5(a) and 5(b) illustrate the distribution of carrier charge density and the electrical characters of metal-oxide-semiconductor junction across the pn junction, respectively. The observed current ratio between the p and n regions was a factor of 10 for positive bias due to the large difference in dopant density, which is 4 orders of magnitude smaller in the

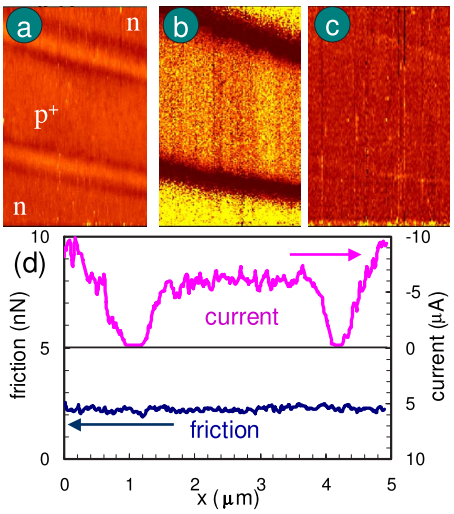

FIG. 4. (Color online) (a) 3.5×5.0 μm topographic, (b) current, and (c) friction images across the silicon pn junction at −4 V bias. The p region is reverse biased, and the n region forward biased. (d) Line profiles of current and friction across the pn junction. [Reprinted with permission from Science (http://www.aaas.org), Ref. 15. Copyright 2006 AAAS.]

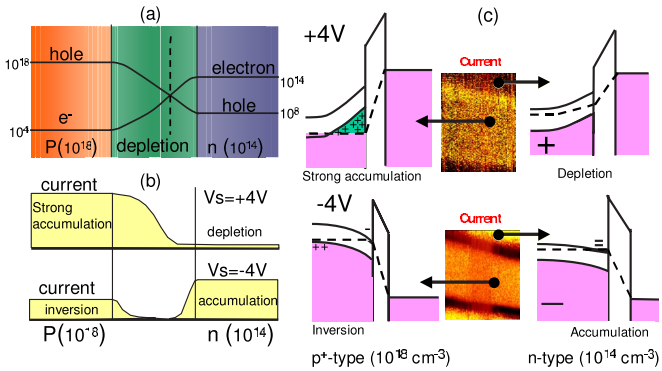

FIG. 5. (Color online) (a) Schematic illustration of the distribution of carrier charge density across the pn junction. (b) Electronic state of metal-oxide-semiconductor junction. V_s refers to the bias of the sample relative to the tip. (c) Band structure of the tip-insulator-semiconductor junctions over both the p and n regions for sample biases of +4 and −4 V.

n region than in the p region (forward bias at heavily doped p region versus reverse bias at low doped n region). For negative bias, the current ratio between the p and n regions for negative bias was only a factor of 2 (reverse bias at heavily doped p region versus the forward bias at low doped n region). Figure 5(c) shows the energy band diagram of the tip-insulator-semiconductor junctions over both the p and n regions for the sample biases of +4 and −4 V. Since the majority carrier in the p (n) region are holes (electrons), a positive sample bias corresponds to forward (reverse) bias of the metal-insulator-semiconductor junction formed by the tip, oxide layer (insulator), and the silicon substrate.[30] At the sample of +4 V in the p region, a large density of majority carrier (holes) is accumulated at the interface due to the high dopant density, resulting in strong inversion, as shown in Fig. 5(c).

In addition to the changes in carrier density, a more trivial effect of the bias voltage is to increase the attractive force between the tip and sample due to the electrostatic force. This contributes in an obvious way to the increase in friction. The effect could be easily and quantitatively taken into account by measuring the change in tip-sample pull-off force as a function of voltage in the p and n regions. Figure 6(a) shows the force experienced by the tip as a function of distance to the sample measured over the n region with sample biases of 0 and −5 V. The force-distance curve at −5 V reveals the attraction before contact due to the long-range electrostatic force. The difference between the pull-off force at −5 and 0 V is due to the electrostatic force. Figure 6(b) shows a plot of the pull-off force as a function of sample bias for the n and p regions. Each data point is the average of five independent measurements and the error bar is associated with the standard deviation of the measurements. As shown in Fig. 6(b), the change of pull-off force with bias increases in proportion to V^2 as expected,[31] with no significant difference between the p and n regions. This is due to the fact that the dielectric constant is high enough in both p and n regions (>10) to make the difference in image charge negligible.

Figure 7(a) shows a color coded friction map (red=high friction; dark=low friction) across the pn junction as a func-

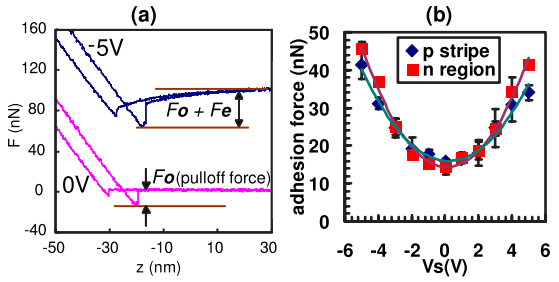

FIG. 6. (Color online) (a) Force-distance curves measured in the *n* region with the sample biases of 0 and −5 V. (b) Plot of the pull-off force as a function of sample bias for both *p* and *n* regions. The error scales represent the standard deviation from five independent measurements. [Reprinted with permission from Science (http://www.aaas.org), Ref. 15. Copyright 2006 AAAS.]

tion of the applied load at +4 V sample bias. In this experiment, the friction force is measured, while the tip is scanning back and forth across the two regions (*y* axis) and while the load is increased stepwise from line to line (*x* axis). A clear enhancement of the friction force in the *p* region as compared to the *n* region is visible. Figure 7(b) is a plot of the friction force versus load at +4 V sample bias. No such enhancement is observed when the bias is negative. The line through the friction data in Fig. 7(b) is a DMT fit. While the agreement with the DMT curve is very good in the *n* region, the *p* region shows a significant "excess" friction. The excess friction in the *p* region is found to be proportional to (total load)$^{\alpha}$, where α is between 2.5 and 3.

Figure 8(a) shows plots of friction and current versus the tip-sample bias measured at the *p* and *n* regions. Each data point is an average of 256 line profiles. As shown in the top and bottom graphs, high current and excess friction are observed for bias $>+2$ V. The line through the friction data shows the parabolic increase in friction calculated from the change in electrostatic force. As can be seen, the increase in friction with bias in the *n* region and in both regions for negative bias is purely the result of the increase in electrostatic force. Above +2 V, the *p* region is in strong accumulation and shows excess friction, in addition to the electrostatic force contribution. The increasing current in the *p* region reflects the rapid increase in carrier density with forward bias.

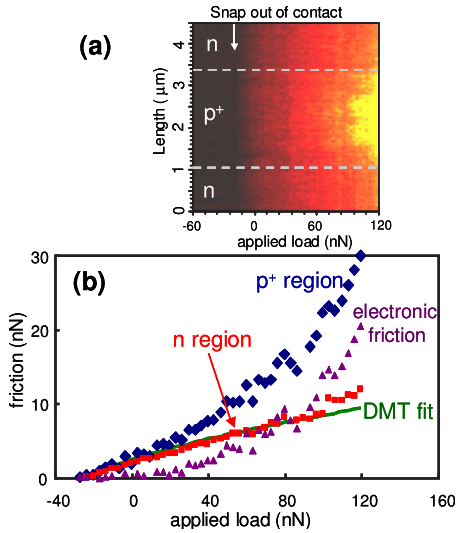

FIG. 7. (Color online) (a) Friction map across the *pn* junction as a function of applied load at +4 V sample bias. In this map, the tip scans repeatedly along one direction only (the *y* axis), while the bias voltage is increased stepwise in each scan line. (b) Plot of the friction force versus load at +4 V sample bias. [Reprinted with permission from Science (http://www.aaas.org), Ref. 15. Copyright 2006 AAAS.]

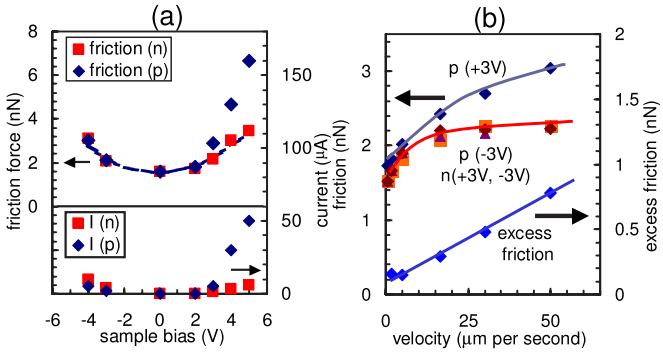

FIG. 8. (Color online) (a) Friction force (top) and current (bottom) in the *p* and *n* regions as a function of sample bias (scanning speed=50 μm/s; load=8 nN). The line is a parabola describing the increase in friction force in the *n* region due to the increase in electrostatic force [obtained using the inset of Fig. 3(a)]. Each data point is the average of 256 line profiles. (b) Plot of friction force as a function of scanning speed (load=8 nN). The lines are guides drawn to highlight the trends in the data. Each data point is the average of 256 line profiles. The difference (excess friction) is a linear function of velocity (bottom curve).

Figure 8(b) shows the velocity dependence of the friction force. In accumulation, the excess friction increased approximately linearly through the velocity range accessible in AFM, while for the *n* region and for the *p* region in reverse bias, a small initial increase was followed by much weaker velocity dependence.

Experiments were conducted to determine if the excess friction was associated with wear or plastic deformation of the surface, which might result from chemical reactions associated with the flowing electrical current, for example, electron-assisted bond breaking at the interface. Plastic deformation could result in changes in adhesion[32] and friction force.[23] Repeated scanning in an area containing both *p* and *n* regions at both positive and negative bias voltages, however, failed to produce any visible wear scar in the AFM images. Since wear leading to topographic changes in height of 0.1 nm or more would have been visible in our images, we can conclude that no wear was produced at the loads and currents used in these experiments.

Another effect of the current could be an increase of temperature. This increase, if present, should decrease, not increase, friction, as shown in recent works.[33–35] For the current and voltages used here, however, the temperature increase should be negligible based on simple calculations of thermal transport.[36]

Finally, we explored the effects of tip passivation, which we achieved by intentionally coating the tip with an insulat-

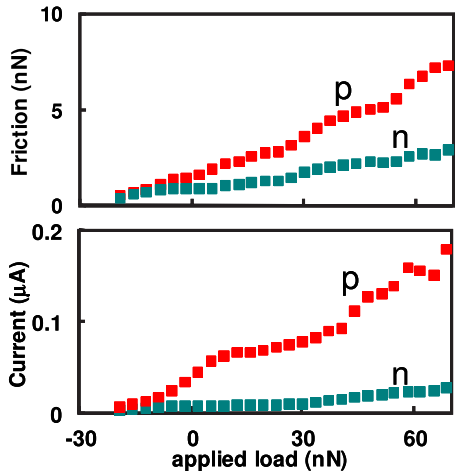

FIG. 9. (Color online) Friction force and current in the p and n regions as a function of applied load at +4 V sample bias measured using tips passivated with an insulating molecular film of hexadecylthiol molecules. Although the current decreased by a factor of 10^3 relative to the clean tip case, the friction force ratio in the p regions remains higher than that in the n region by a factor of 1.6.

ing molecular film of hexadecylthiol molecules. To accomplish this, the tip was rubbed against a gold sample covered with an hexadecylthiol monolayer that was previously stored in the vacuum system.[37,38] The tip-sample current after this procedure decreased by a factor of $\sim 10^3$.[39] Although the friction force decreased in both n and p regions for all bias voltages due to the lubricating properties of the hexadecylthiol, excess friction was still observed in strong accumulation. Figure 9 shows plots of friction and current versus applied load measured at p and n regions. For example, at an applied load of 8 nN and a sample bias of +4 V, the friction force with the uncoated metallic probe was 4.7 nN in the p region versus 3.0 nN in the n region [see Fig. 3(b)], a ratio of 1.6. For the thiol-coated tip at the same load, the contributions were 3.1 nN and 1.5 nN, a ratio of 2.0. This result reveals that the excess friction is not directly associated with the tip-sample current. Therefore, current induced effects such as local heating or chemical modification are not responsible for the excess friction. The factor which influences the excess friction is the surface carrier density caused by the electrostatic field at the tip-sample proximity.

IV. DISCUSSION

We can compare the excess friction observed in our experiments with experimental and theoretical investigations of electronic contributions to friction in other systems. Electronic dissipation processes are manifested in many phenomena, for example, in an increased film resistivity caused by scattering of electrons by adsorbates,[6] in the appearance of antiabsorption peaks in infrared spectra for dipole-forbidden adsorbate vibrations,[8] and in the broadening of adsorbate vibrational lines.[7,11] In a different kind of experiment, Dayo *et al.*[12] measured frictional dissipation for N_2 molecules sliding over a lead film using a quartz crystal microbalance. Friction decreased upon crossing the superconducting transition temperature of the lead substrate[12,40] and was attributed to the suppression of electronic excitations in the superconducting substrate,[14] an interpretation that is currently being debated.[41,42] The origin and magnitude of the friction forces acting on individual molecules have been reviewed by Persson.[1] If the relative velocity between substrate and adsorbate is much smaller than the speed of sound and the Fermi velocity of the substrate electrons, then the electronic friction force acting on a molecule is given by $F_e = v\Gamma_{\text{atom}}$, where Γ_{atom} is the viscosity friction coefficient and v is the relative velocity between substrate and adsorbate.

As shown in Fig. 3(c), we observed 1 nN excess friction for tip-sample velocities of 50 μm/s at a sample bias of +3 V, leading to a dissipation Γ_{tip} of $\sim 2 \times 10^{-5}$ N s/m. Frictional dissipation in metallic and semiconductor surfaces has recently been investigated in AFM experiments.[43–45] Stipe *et al.*[44] observed dissipation when a gold tip moved parallel to a gold surface. Dissipation increased approximately as the inverse of the tip-sample distance and as the square of the bias. At room temperature and near-zero bias, they observed Γ_{tip} of $\sim 10^{-12}$ N s/m at 2.5 nm from the surface. Dorofeyev *et al.*[43] measured the tip-sample dissipation through observation of thermal fluctuations for an Al-coated tip moving perpendicular to a gold surface, obtaining $\Gamma_{\text{tip}} \sim 4 \times 10^{-9}$ N s/m for near-zero bias just before jump to contact. Volokitin and Persson have analyzed dissipation for a metallic tip moving close to a surface.[45] For clean conductors and a parabolic tip apex, they estimate an upper limit to the electronic friction of $\Gamma_{\text{tip}} < \sim 10^{-15}$ N s/m; however, in the presence of adsorbates that can vibrate with acoustical modes parallel to the surface, this value increased to 7×10^{-13}. Joule dissipation associated with dragging the carrier charges[46] was also considered and found to be below 10^{-11} N s/m.

The noncontact friction results of Kuehn *et al.* on polymer films on gold were attributed to electric field fluctuations and were modeled using the fluctuation-dissipation theorem.[47,48] If we extrapolate the values of Kuehn *et al.* using their finding that Γ varies approximately as V^2/d, to our parameter values ($V = 2-4$ V; $d = 0.3$ nm), we obtain $\Gamma = 10^{-8}-10^{-9}$ N s/m. In our case, the fluctuations might originate from charging and discharging of traps in the thin SiO_2 layer due to the large accumulation in the highly doped p-Si substrate, and these could be larger than in the case of the polymer films. The experiments on various thickness of the oxide layer could be an intriguing attempt to test this possibility.

The excess friction in the p region during accumulation increases significantly with contact stress but is not related to wear. It is not proportional to the tip-sample current either, which excludes chemical effects as the potential origin. Previous calculations of electronic friction do not include the effects of localized strain under the AFM tip at approximately gigapascal levels, and this may also play a role in excess friction, perhaps by creating additional electronic surface states that are charged and then discharged upon release of the stress.

Another interesting effect worthy of consideration is that in the pressure range of gigapascals, a decrease of the band gap occurs,[49] which in our geometry should produce a pressure-induced quantum dot under the tip. This could lead

to a substantial enhancement of electron-hole recombination, with the energy emitted in the form of phonons or photons. Another possibility to be discussed is the enhancement of dislocation mobility due to the increase in charge carrier density. Such an effect, shown by Patel *et al.*,[50] might also explain the appearance of excess friction. It is not clear, however, that a substantial amount of dislocations are present or created in the small area of the tip contact to account for the magnitude of the observed effect.

Although more experiments and a more thorough theoretical investigation are necessary for a satisfactory understanding of our findings, the phenomenon might have interesting technological applications for microelectromechanical devices and in the motion of nano-objects in patterned semiconductor substrates. The ability to modulate friction through control of doping levels and electric fields offers new and interesting possibilities.

V. CONCLUSION

In conclusion, using a Si (100) sample patterned with *p* and *n* regions with large differences in doping levels, we have shown that the nanoscale friction properties can be manipulated significantly by the simple application of a bias voltage. By varying the bias between the tip and sample, charge depletion or accumulation could be induced in the *n* and *p* regions, which resulted in significant differences in the friction force. The results of many types of experiments (bias voltage and sign, velocity, and tip passivation) are consistent with the existence of a substantial electronic influence on the friction force. In addition, we have shown that using semiconductor materials whose electronic properties can be manipulated by application of bias voltages, this friction contribution can be adjusted in a controlled way. This offers an interesting way of tuning or switching the frictional response in nanoscale devices.

ACKNOWLEDGMENTS

This work was supported by the Director, Office of Energy Research, Office of Basic Energy Sciences, Materials Sciences Division, of the U.S. Department of Energy through the Lawrence Berkeley National Laboratory, Contract No. DE-AC02-05CH11231, and through the Ames Laboratory, Contract No. W-405-Eng-82. We thank R. J. Phaneuf of the Department of Materials Science and Engineering, University of Maryland for kindly providing the patterned Si samples.

*Authors to whom correspondence should be addressed.
†jypark@lbl.gov
‡mbsalmeron@lbl.gov

[1] B. N. J. Persson, *Sliding Friction: Physical Principles and Applications* (Springer-Verlag, Berlin, 1998).
[2] R. W. Carpick and M. Salmeron, Chem. Rev. (Washington, D.C.) **97**, 1163 (1997).
[3] E. Gnecco, R. Bennewitz, T. Gyalog, and E. Meyer, J. Phys.: Condens. Matter **13**, R619 (2001).
[4] G. A. Tomlinson, Philos. Mag. **7**, 905 (1929).
[5] A. Socoliuc, R. Bennewitz, E. Gnecco, and E. Meyer, Phys. Rev. Lett. **92**, 134301 (2004).
[6] B. N. J. Persson, Phys. Rev. B **44**, 3277 (1991).
[7] B. N. J. Persson, E. Tosatti, D. Fuhrmann, G. Witte, and C. Woll, Phys. Rev. B **59**, 11777 (1999).
[8] B. N. J. Persson and A. I. Volokitin, Surf. Sci. **310**, 314 (1994).
[9] M. Headgordon and J. C. Tully, J. Chem. Phys. **103**, 10137 (1995).
[10] J. C. Tully, M. Gomez, and M. Headgordon, J. Vac. Sci. Technol. A **11**, 1914 (1993).
[11] G. Witte, K. Weiss, P. Jakob, J. Braun, K. L. Kostov, and C. Woll, Phys. Rev. Lett. **80**, 121 (1998).
[12] A. Dayo, W. Alnasrallah, and J. Krim, Phys. Rev. Lett. **80**, 1690 (1998).
[13] J. Krim, Phys. Rev. Lett. **83**, 1262 (1999).
[14] M. Highland and J. Krim, Phys. Rev. Lett. **96**, 226107 (2006).
[15] J. Y. Park, D. F. Ogletree, P. A. Thiel, and M. Salmeron, Science **313**, 186 (2006).
[16] J. Y. Park and R. J. Phaneuf, J. Vac. Sci. Technol. B **21**, 1254 (2003).
[17] J. Jahanmir, P. E. West, A. Young, and T. N. Rhodin, J. Vac. Sci. Technol. A **7**, 2741 (1989).
[18] A. Ishizaka and Y. Shiraki, J. Electrochem. Soc. **133**, 666 (1986).
[19] J. Y. Park and R. J. Phaneuf, Appl. Phys. Lett. **82**, 64 (2003).
[20] J. Y. Park, E. D. Williams, and R. J. Phaneuf, J. Appl. Phys. **91**, 3745 (2002).
[21] RHK Technology, Troy, MI, model No. UHV-350.
[22] J. Y. Park, D. F. Ogletree, M. Salmeron, C. J. Jenks, and P. A. Thiel, Tribol. Lett. **17**, 629 (2004).
[23] J. Y. Park, D. F. Ogletree, M. Salmeron, R. A. Ribeiro, P. C. Canfield, C. J. Jenks, and P. A. Thiel, Phys. Rev. B **71**, 144203 (2005).
[24] NT-MDT Co., Zelenograd Research Institute of Physical Problems, Moscow, Russia.
[25] J. E. Sader, J. W. M. Chon, and P. Mulvaney, Rev. Sci. Instrum. **70**, 3967 (1999).
[26] D. F. Ogletree, R. W. Carpick, and M. Salmeron, Rev. Sci. Instrum. **67**, 3298 (1996).
[27] The relation between the contact area and applied load can be described by the Derjaguin-Muller-Toporov (DMT) or the Johnson-Kendall-Roberts (JKR) model, depending on the adhesion force and hardness of the sample. Generally, the JKR model is appropriate for soft materials with large adhesion, while DMT applies best in the case of high stiffness and low adhesion.
[28] J. Y. Park, R. J. Phaneuf, D. F. Ogletree, and M. Salmeron, Appl. Phys. Lett. **86**, 172105 (2005).
[29] M. Enachescu, R. J. A. van den Oetelaar, R. W. Carpick, D. F. Ogletree, C. F. J. Flipse, and M. Salmeron, Phys. Rev. Lett. **81**, 1877 (1998).
[30] S. M. Sze, *Physics of Semiconductor Devices* (Wiley, New York, 1981).
[31] B. M. Law and F. Rieutord, Phys. Rev. B **66**, 035402 (2002).

[32] J. Y. Park, D. F. Ogletree, M. Salmeron, R. A. Ribeiro, P. C. Canfield, C. J. Jenks, and P. A. Thiel, Philos. Mag. **86**, 945 (2006).

[33] E. Gnecco, R. Bennewitz, T. Gyalog, C. Loppacher, M. Bammerlin, E. Meyer, and H. J. Guntherodt, Phys. Rev. Lett. **84**, 1172 (2000).

[34] S. Y. Krylov, K. B. Jinesh, H. Valk, M. Dienwiebel, and J. W. M. Frenken, Phys. Rev. E **71**, 065101(R) (2005).

[35] E. Riedo and E. Gnecco, Nanotechnology **15**, S288 (2004).

[36] Thermal transport calculations using the thermal conductivity of silicon $k=1.5$ W/(cm K), a current of 10 μA, at 4 V bias, and a tip radius of 100 nm show an increase of temperature of less than 1 °C.

[37] L. Howald, R. Luthi, E. Meyer, and H. J. Guntherodt, Phys. Rev. B **51**, 5484 (1995).

[38] J. Y. Park, D. F. Ogletree, M. Salmeron, R. A. Ribeiro, P. C. Canfield, C. J. Jenks, and P. A. Thiel, Science **309**, 1354 (2005).

[39] J. Y. Park, D. F. Ogletree, M. Salmeron, R. A. Ribeiro, P. C. Canfield, C. J. Jenks, and P. A. Thiel, Phys. Rev. B **74**, 024203 (2006).

[40] B. L. Mason, S. M. Winder, and J. Krim, Tribol. Lett. **10**, 59 (2001).

[41] B. N. J. Persson and E. Tosatti, Surf. Sci. **411**, L855 (1998).

[42] R. L. Renner, J. E. Rutledge, and P. Taborek, Phys. Rev. Lett. **83**, 1261 (1999).

[43] I. Dorofeyev, H. Fuchs, G. Wenning, and B. Gotsmann, Phys. Rev. Lett. **83**, 2402 (1999).

[44] B. C. Stipe, H. J. Mamin, T. D. Stowe, T. W. Kenny, and D. Rugar, Phys. Rev. Lett. **87**, 096801 (2001).

[45] A. I. Volokitin and B. N. J. Persson, Surf. Sci. **587**, 88 (2005).

[46] W. Denk and D. W. Pohl, Appl. Phys. Lett. **59**, 2171 (1991).

[47] S. Kuehn, R. F. Loring, and J. A. Marohn, Phys. Rev. Lett. **96**, 156103 (2006).

[48] S. Kuehn, J. A. Marohn, and R. F. Loring, J. Phys. Chem. B **110**, 14525 (2006).

[49] X. J. Zhu, S. Fahy, and S. G. Louie, Phys. Rev. B **39**, 7840 (1989).

[50] J. R. Patel, L. R. Testardi, and P. E. Freeland, Phys. Rev. B **13**, 3548 (1976).